Inorg. Chem. **1996,** *35,* 3039−3043 **3039**

Electronic Structure of *π*-Conjugated Redox Systems with Borane/Borataalkene End Groups

Jan Fiedler and Stanislav Zališ

J. Heyrovsky Institute of Physical Chemistry, Academy of Sciences of the Czech Republic,
Dolejškova 3, CZ-18223 Prague, Czech Republic

Axel Klein, Fridmann M. Hornung, and Wolfgang Kaim*

Institut für Anorganische Chemie der Universität, D-70550 Stuttgart, Germany

Received November 17, 1995[⊗]

The compounds 1,4-bis(dimesitylboryl)benzene (**1**), 4,4′-bis(dimesitylboryl)biphenyl (**2**), and dimesitylphenylborane (**3**) were studied by UV/vis/near-IR spectroelectrochemistry. In contrast to the colorless precursor compounds, all negatively charged species $\mathbf{1}^{\bullet-/2-}$, $\mathbf{2}^{\bullet-/2-}$, and $\mathbf{3}^{\bullet-}$ exhibit intense long-wavelength absorption maxima in the visible or near-infrared region, e.g., at 1305 nm ($\epsilon = 31\,200$ M^{-1} cm^{-1}; $\mathbf{2}^{\bullet-}$) or at 736 nm ($\epsilon = 67\,700$ M^{-1} cm^{-1}; $\mathbf{2}^{2-}$). The absorption bands of the organoborane anion radicals and their appearance, including their vibrational structuring, resemble those of corresponding amine radical cations such as Wurster's Blue. The conformation of the dimesitylboryl substituent toward a phenyl ring was established using the crystal structure results for **3** ($C_{24}H_{27}B$, monoclinic, space group *C*2/*c*, $a = 13.324(3)$ Å, $b = 9.143(2)$ Å, $c = 16.303(3)$ Å, $\beta = 98.93(3)°$, $V = 1962.0(7)$ Å^3, $Z = 4$, $R = 0.0493$). *Ab initio* calculations (6-31G**) on the BH_2-substituted analogues of **1**−**3** and on **3** proper confirmed the concept of an increasingly quinonoid distortion of the organoboron redox systems on reduction and served in assigning the observed electronic transitions. A 23−35% participation of the boron *π* centers at the lowest unoccupied MOs is in agreement with results from EPR/ENDOR measurements of the radical intermediates, indicating sizable contributions from the diboratasemiquinone or—in the extreme—from delocalized B^{III}/B^{II} mixed-valent formulations in the bifunctional compounds $\mathbf{1}^{\bullet-}$ and $\mathbf{2}^{\bullet-}$.

Redox systems based on conjugated organonitrogen compounds[1] are well-established in many areas which require reversible outer-sphere electron transfer reactivity.[1,2] Among the most familiar and frequently used examples are the 1,1′-dialkyl-4,4′-bipyridinium ("methylviologen")[1,2] and the *N*,*N*,*N*′,*N*′-tetraalkyl-*p*-phenylenediamine or -benzidine systems (Scheme 1).[1,3]

Applying the concept of isoelectronic compounds and redox series,[4] we have previously pointed out the existence of analogous redox systems (Scheme 2) based on $-BR_2/-BR^{\bullet-}/{=}BR_2^-$ instead of $-NR_2/-NR_2^{\bullet+}/{=}NR_2^+$ as essential end groups of conjugated *π* systems.[5] The corresponding redox series then involve anionic charges instead of cationic ones (Scheme 1) and the cationic quinonediiminium forms correspond to anionic diborataquinonoid systems with borataalkene (alkylideneborate) structures.

To obtain persistent examples of organoboron redox systems as in Scheme 2, we have cicumvented the problem of coordinative unsaturation at boron by using two mesityl substituents (Scheme 2, R = Mes) in compounds **1** and **2**. Mesityl substituents as in dimesitylboryl groups[5−7] or other compounds[8] are well-suited to protect axial positions against attack at p_z[5−7] or d_{z^2} orbitals.[8]

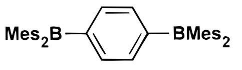

1

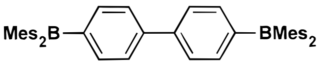

2

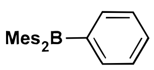

3

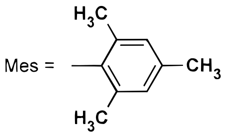

Electrochemical studies of the redox systems $\mathbf{1}^{0/\bullet-/2-}$ and $\mathbf{2}^{0/\bullet-/2-}$ have provided first indications for the validity of the N/B analogy (Schemes 1 and 2) by showing two well-separated one-electron reduction processes of the neutral precursors.[5] The smaller system exhibits a higher stability range of the para-

---

[⊗] Abstract published in *Advance ACS Abstracts*, April 15, 1996.

(1) Deuchert, K.; Hünig, S. *Angew. Chem.* **1978**, *90*, 927; *Angew. Chem., Int. Ed. Engl.* **1978**, *17*, 875.

(2) (a) Hünig, S.; Berneth, H. *Top. Curr. Chem.* **1980**, *92*, 1. (b) Bird, C. L.; Kuhn, A. T. *Chem. Soc. Rev.* **1981**, *10*, 49.

(3) Michaelis, L. *Chem. Ber.* **1935**, *16*, 243.

(4) Kaim, W. *Angew. Chem.* **1980**, *92*, 940; *Angew. Chem., Int. Ed. Engl.* **1980**, *19*, 911.

(5) (a) Kaim, W.; Schulz, A. *Angew. Chem.* **1984**, *96*, 611; *Angew. Chem., Int. Ed. Engl.* **1984**, *23*, 615. (b) Schulz, A.; Kaim W. *Chem. Ber.* **1989**, *122*, 1863.

(6) (a) Bartlett, R. A.; Power, P. P. *Organometallics* **1986**, *5*, 1916. (b) Yuan, Z.; Taylor, N. J.; Marder, T. B.; Williams, I. D.; Kurtz, S. K.; Cheng, L.-T. *J. Chem. Soc., Chem. Commun.* **1990**, 1489. (c) Moezzi, A.; Olmstead, M.; Power, P. P. *J. Am. Chem. Soc.* **1992**, *114*, 2715. (d) Okada, K.; Sugawa, T.; Oda, M. *J. Chem. Soc., Chem. Commun.* **1992**, 74. (e) Pestanan, D. C.; Power, P. P. *Organometallics* **1992**, *11*, 98. (f) Moezzi, A.; Olmstead, M. M.; Bartlett, R. A.; Power, P. P. *Organometallics* **1992**, *11*, 2383. (g) Olmstead, M. M.; Power, P. P. *J. Am. Chem. Soc.* **1986**, *108*, 4235. (h) Okada, K.; Kawata, T.; Oda, M. *J. Chem. Soc., Chem. Commun* **1995**, 233. (i) Okada, K.; Suzuki, R.; Oda, M. *J. Chem. Soc., Chem. Commun.* **1995**, 2069.

(7) Glogowski, M. E.; Grisdale, P. J.; Williams, J. L. R.; Reagan, T. H. *J. Organomet. Chem.* **1973**, *54*, 51. (b) Glogowski, M. E.; Williams, J. L. R. *J. Organomet Chem.* **1980**, *195*, 123. (c) Glogowski, M. E.; Williams, J. L. R. *J. Organomet. Chem.* **1981**, *216*, 1. (d) Glogowski, M. E.; Zumbulyadis, N.; Williams, J. L. R. *J. Organomet. Chem.* **1981**, 231, 97. (e) Pelter A.; Singaram, B.; Williams, L.; Wilson, J. W. *Tetrahedron Lett.* **1983**, 623. (f) Pelter, A.; Singaram, S.; Brown, H. C. *Tetrahedron Lett.* **1983**, 1433. (g) Pelter, A.; Buss, D.; Colclough, E. *J. Chem. Soc., Chem. Commun.* **1987**, 297. (h) Cardin C. J.; Parge, H. E.; Wilson J. W. *J. Chem. Res. (S)* **1983**, 93.

S0020-1669(95)01482-0 CCC: $12.00

Scheme 1

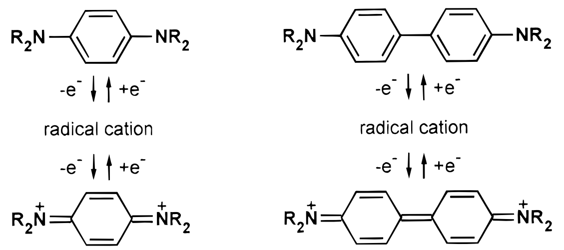

Scheme 2

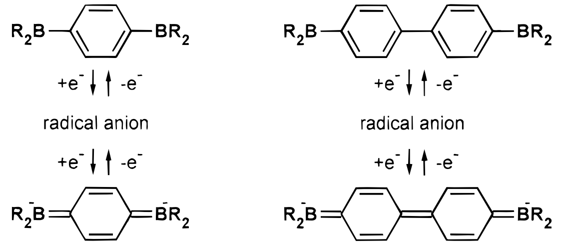

Scheme 3

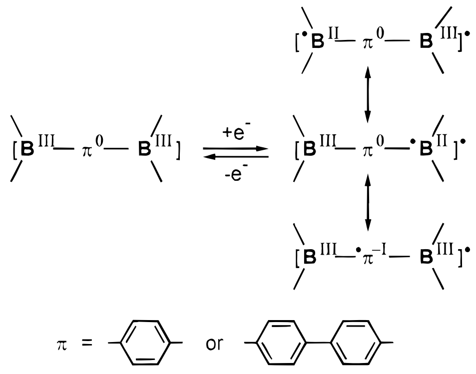

magnetic intermediate and a less negative potential for the first reduction, thus indicating a very strong substituent effect.[5b] As supporting evidence, EPR/ENDOR studies[5] revealed low π spin populations at the CH π centers and correspondingly larger amounts of π spin population at the boron atoms which led to possible resonance formulations of the reduced forms involving a delocalized B^{III}/B^{II} mixed-valent situation (Scheme 3).[5b]

The conspicuous intense colors observed for the reduced species in the redox series from Scheme 2 (R = Mes) have prompted us now to investigate these diborane systems and the monoborane $PhBMes_2$ (**3**)[5b,6h] by UV/vis/near-IR spectroelectrochemistry. Absorption spectra of radical ions[9−11] reveal much additional information on their electronic structure, in particular, when supported by quantum-chemical calculations.[11] On the basis of data from experiments and calculations, we shall propose assignments of transitions and assess the contributions from resonance structures. These results will be put into perspective by comparing them with those of corresponding nitrogen derivatives, i.e., the radical cations[9,10] of *N*,*N*,*N*′,*N*′-tetramethyl-*p*-phenylenediamine (**4**$^{\bullet+}$, Wurster's Blue) and -benzidine (**5**$^{\bullet+}$) (cf. Scheme 1, R = CH_3) and of closely related boron−nitrogen (**6, 7**)[12] or all-carbon systems such as Thiele's (**8**) and Chichibabin's hydrocarbons (**9**).[13]

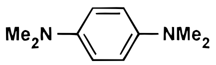

4

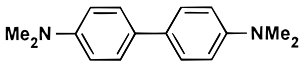

5

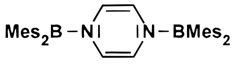

6

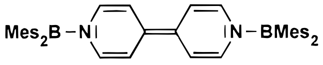

7

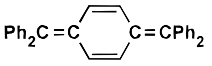

8

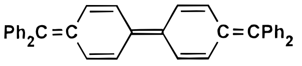

9

To support the interpretation of spectroelectrochemical results, we have determined the molecular structure of $PhBMes_2$ in the crystal. The angles between the aryl groups and the central BC_3 plane are particularly interesting since the aryldimesitylborane entity is common to all systems **1**−**3**. *Ab initio* calculations were performed for **3** and for BH_2-substituted model compounds (**11**−**13**) (Scheme 2: R = H) in order to estimate the participation of the boron π centers at the relevant frontier orbitals and to aid in the assignment of electronic transitions.

Experimental Section

Materials and Instrumentation. The syntheses of the compounds 1,4-bis(dimesitylboryl)benzene (**1**), 4,4′-bis(dimesitylboryl)biphenyl (**2**), and dimesitylphenylborane (**3**) were described earlier.[5]

UV/vis/near-IR absorption spectra were recorded on a Bruins Instruments Omega 10 spectrophotometer. Spectroelectrochemical measurements were performed in THF/0.1 M Bu_4NPF_6 (THF = tetrahydrofuran) solutions using an optically transparent thin-layer electrode (OTTLE) cell:[14] path length 0.15 mm, Pt minigrid working electrode, Pt grid auxiliary electrode, Ag wire reference electrode. THF was freshly distilled from potassium, all manipulations were performed under argon using Schlenk or syringe techniques.

X-ray Structure Determination. Single crystals of compound **3** were obtained by cooling a saturated solution in *n*-hexane to −20 °C. The crystal used for diffraction was a colorless plate of dimensions 0.8 mm × 0.3 mm × 0.1 mm, which was taken from the mother liquor, separated under nujol, and sealed in a glass capillary. The 2355 independent reflections (2984 measured reflections, $R_{int} = 0.0668$; $5.06° < 2\theta < 56.0°$; $h = -1$ to $+17$; $k = -1$ to $+12$; $l = -21$ to $+21$) were measured at 188 K on a Siemens-P4 diffractometer using monochromatized Mo Kα radiation (Table 1). There was no absorption correction due to the absence of heavy atoms. The structure was solved in the space group *C*2/*c* by direct methods using the SHELXTL-PLUS package;[15a] the refinement was carried out with SHELXL-93,[15b] employing full-matrix least-squares methods. Anisotropic thermal parameters were refined for all non-hydrogen atoms. The C−H aromatic hydrogen atoms were located; methyl hydrogen atoms were placed in their ideal positions and allowed to ride on the corresponding

---

(8) (a) Kaim W.; Klein, A. *Organometallics* **1995**, *14*, 1176. (b) Klein, A.; Kaim, W.; Waldhör, E.; Hausen, H.-D. *J. Chem. Soc., Perkin Trans. 2* **1995**, 2121.

(9) Shida, T. *Electronic Absorption Spectra of Radical Ions*; Elsevier: Amsterdam, 1988; (a) p 211; (b) p 220; (c) p 223.

(10) (a) Sakata, T.; Nagakura, S. *Bull. Chem. Soc. Jpn.* **1970**, *43*, 2414. (b) Takemoto, K.; Matsusaka, H.; Nakayama, S.; Suzuki, K.; Ooshika, Y. *Bull. Chem. Soc. Jpn.* **1968**, *41*, 764.

(11) (a) Braterman, P. S.; Sony, J.-I.; Kohlmann, S.; Vogler, C.; Kaim, W. *J. Organomet. Chem.* **1991**, *411*, 207. (b) Krejcik, M.; Zalis, S.; Ladwig, M.; Matheis, W.; Kaim, W. *J. Chem. Soc., Perkin Trans. 2* **1992**, 2007. (c) Hilgers, F.; Kaim, W.; Schulz, A.; Zalis, S. *J. Chem. Soc., Perkin Trans. 2* **1994**, 135. (d) Matheis, W.; Poppe, J.; Kaim W.; Zalis, S *J. Chem. Soc., Perkin Trans. 2* **1994**, 1923. (e) Braterman, P. S.; Song, J.-I. *J. Org. Chem.* **1991**, *56*, 4678.

(12) (a) Lichtblau, A.; Hausen, H.-D.; Schwarz, W.; Kaim, W. *Inorg. Chem.* **1993**, *32*, 73. (b) Lichtblau, A.; Kaim, W.; Schulz, A.; Stahl, T. *J. Chem. Soc., Perkin Trans. 2* **1992**, 1497.

(13) Montgomery, L. K.; Huffman, J. C.; Jurczak, E. A.; Grendze, M. P. *J. Am. Chem. Soc.* **1986**, *108*, 6004.

(14) (a) Krejcik, M.; Vlcek, A. A. *J. Electroanal. Chem. Interfacial Electrochem.* **1991**, *313*, 243. (b) Krejcik, M.; Danek M.; Hartl, F. *J. Electroanal Chem. Interfacial Electrochem.* **1991**, *317*, 179.

(15) (a) Sheldrick, G. M. *SHELXTL-PLUS: An Integrated System for Solving, Refining and Displaying Crystal Structures from Diffraction Data*; Siemens Analytical X-Ray Instruments Inc.: Madison, WI, 1989. (b) Sheldrick, G. M. *SHELXL-93, Program for Crystal Structure Determination*; Universität Göttingen: Göttingen, Germany, 1993.

Table 1. Crystallographic Data for $PhBMes_2$

empirical formula	$C_{24}H_{27}B$	Z	4
fw, g/mol	326.27	T, °C	−85
space group	$C2/c$ [No. 15]	λ, Å	0.71073 Å
a, Å	13.324(3)	ρ_{calcd}, g cm^{-3}	1.105
b, Å	9.143(2)	μ, cm^{-1}	0.610
c, Å	16.303(3)	R^a [$I > 2\sigma(I)$]	0.0496
β, deg	98.93(3)	$R_w{}^b$	0.1432
V, Å^3	1962.0(7)	GOF^c	0.864

^{a} $R = (\Sigma||F_o| - |F_c||)/\Sigma|F_o|$. ^{b} $R_w = \{\Sigma[w(|F_o|^2 - |F_c|^2)^2]/\Sigma[w(F_o{}^4)]\}^{1/2}$. ^{c} GOF $= \{\Sigma w(|F_o|^2 - |F_c|^2)^2/(n - m)\}^{1/2}$; n = no. of reflections; m = no. of parameters.

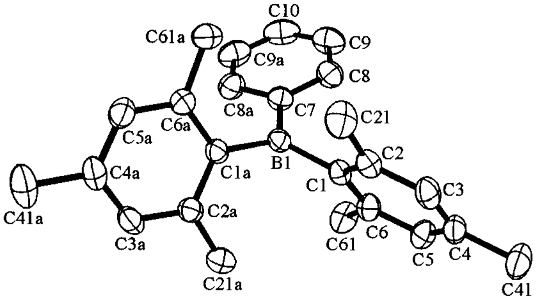

Figure 1. Molecular structure of $PhBMes_2$ (**3**) in the crystal. Selected bond lengths (Å) and angles (deg): B−C1, 1.579(2); B−C7, 1.569(3); C1−B−C7, 118.6(1); C1−B−C1a, 122.8(2). For dihedral angles see text.

carbon atoms. Final refinement converged at $R = 0.0496$ ($I > 2\sigma(I)$) and at $R_w = 0.1432$ (for all data).

Calculations. *Ab initio* calculations using the 6-31G** basis[16a−18] were performed with the GAUSSIAN92 program package;[16b] the restricted HF approach was applied for calculating the open-shell systems. Geometry optimization of the model compounds **12** and $\mathbf{12}^{2-}$ in general C_1 symmetry yielded planar geometries as energy minima. Deviation of the H−B−H planes from the phenyl planes did not qualitatively alter the electronic structure. For the BH_2-substituted model redox systems $\mathbf{11}^{0/\bullet-/2-}$, $\mathbf{12}^{0/\bullet-/2-}$, and $\mathbf{13}^{0/\bullet-/2-}$ we therefore assumed planar configurations with the symmetry constrained to D_{2h} (**11, 12**) or C_{2v} (**13**). *Ab initio* and AM1[16c] calculations of **3** and **13** confirmed the relatively small perturbation caused by replacing Mes through H.

Results

Structure. To establish the conformational preference in the systems investigated, we determined the crystal structure of compound **3** (Table 1) which represents the simplest common motif phenyl-$BMes_2$ for all three compounds **1**−**3**. No significant intermolecular interaction could be found in the crystal of **3**; a structural representation and the main bond lengths and angles are given in Figure 1. A 2-fold symmetry axis runs through boron and the *para* carbon center of the phenyl ring; a similar situation was found for $BMes_3$.[6a] In relation to the plane B1,C1,C1a,C7 around trigonal boron, the phenyl ring exhibits a dihedral angle of $\omega_1 = 21.6(1)°$ and the mesityl rings of $|\omega_2| = 60.57(5)°$. The dihedral angle between the phenyl and mesityl rings is 71.93(5)°.

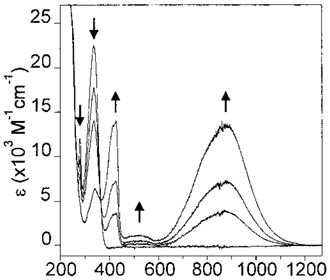

Figure 2. Spectroelectrochemical change for the transition $\mathbf{1}^0 \rightarrow \mathbf{1}^{\bullet-}$ in THF/0.1 M Bu_4NPF_6.

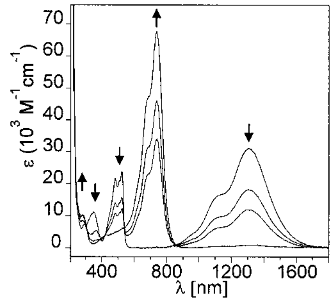

Figure 3. Spectroelectrochemical change for the transition $\mathbf{2}^{\bullet-} \rightarrow \mathbf{2}^{2-}$ in THF/0.1 M Bu_4NPF_6.

Spectroelectrochemistry. According to eqs 1−3, compounds **1**−**3** undergo cyclovoltammetrically reversible one-electron reduction processes at a 100 mV/s scan rate.[5]

$$\mathbf{1} \underset{-e^-}{\overset{+e^-}{\rightleftharpoons}} \mathbf{1}^{\bullet-} \underset{-e^-}{\overset{+e^-}{\rightleftharpoons}} \mathbf{1}^{2-} \tag{1}$$

−1.39 V −2.08 V vs SCE in DMF/0.1 M Bu_4NClO_4

$$\mathbf{2} \underset{-e^-}{\overset{+e^-}{\rightleftharpoons}} \mathbf{2}^{\bullet-} \underset{-e^-}{\overset{+e^-}{\rightleftharpoons}} \mathbf{2}^{2-} \tag{2}$$

−1.47 V −1.72 V vs SCE in DMF/0.1 M Bu_4NClO_4

$$\mathbf{3} \underset{-e^-}{\overset{+e^-}{\rightleftharpoons}} \mathbf{3}^{\bullet-} \tag{3}$$

−1.85 V vs SCE in DMF/0.1 M Bu_4NClO_4

To relate the UV/vis/near-IR spectroelectrochemical results with previous EPR/ENDOR measurements,[5] we performed these experiments in THF/0.1 M Bu_4NPF_6. Under those conditions, the reversibility of the reduction of **3** and of the second reduction of **1** was not 100% complete within the typical time scale of 5 min, the extinction coefficients at the absorption maxima of the corresponding products could thus not be determined with the usual accuracy of ±2%. Figures 2 and 3 show representative spectral changes for the diboranes; Table 2 lists the absorption data.

All three aromatic boranes are colorless in the neutral state. On reduction, the monoborane **3** develops a moderately intense and very broad band with an absorption maximum at 692 nm; $\lambda_{max} = 600$ nm was reported for $\mathbf{1}^{\bullet-}$ formed by reduction with Na/K alloy in THF.[6h] Diboranes **1** and **2** develop intense absorptions in the visible and near-infrared on reduction. Whereas $\mathbf{2}^{\bullet-}$ shows an unusually intense and distinctly split band system in the near-infrared region (Figure 2), the smaller *p*-phenylenediborane derivative $\mathbf{1}^{\bullet-}$ exhibits a broad maximum at 872 nm, accompanied by a high-energy shoulder. On

---

(16) (a) Frisch, M. J.; Pople, J. A.; Binkley, J. S.; *J. Chem. Phys.* **1984**, *80*, 3265. (b) Frisch, M. J.; Trucks, G. W.; Schlegel, H. B.; Gill, P. M. W.; Johnson, B.G.; Wong, M. W.; Foresman, J. B.; Robb, M. A.; Head-Gordon, M.; Replogle, E. S.; Gomperts, R.; Andres, J. L.; Raghavachari, K.; Binkley, J. S.; Gonzalez, C.; Martin, R. L.; Fox, D. J.; Defrees, D. J.; Baker, J.; Stewart, J. J. P.; Pople, J. A. *Gaussian 92/DFT,* Revision G.3; Gaussian, Inc.: Pittsburgh, PA, 1993. (c) Dewar, M. J. S.; Zoebisch, E. G.; Healy, E.F.; Stewart, J. J. P. *J. Am. Chem. Soc.* **1985**, *107*, 3902.

(17) Bertho, D.; Jouanin, C. *Synth. Met.* **1988**, *24*, 179.

(18) Olmstead, M. M.; Power, P. P.; Weese, K. J.; Doedens, R. F. *J. Am. Chem. Soc.* **1987**, *109*, 2541.

Table 2. Absorption Maxima λ_{max} (nm) and Extinction Coefficients ϵ (M^{-1} cm^{-1}) of Boron Compounds[a] and Nitrogen Analogues[b]

compound	λ_{max} (ϵ)
1	337 (22 500)
$\mathbf{1}^{\bullet-}$	872 (13 300), 791(sh); 424 (13 800), 415(sh), 403(sh); 340 (6000)
$\mathbf{4}^{\bullet+\,b}$	637, 578
$\mathbf{1}^{2-}$	665 (≈11 700)[c]
2	342 (48 000)
$\mathbf{2}^{\bullet-}$	1305 (31 200),1127(sh), 996(sh); 522 (23 400), 511(sh), 481 (21 400); 346 (11 000)
$\mathbf{5}^{\bullet+\,b}$	1075, 925, 820; 468, 453, 435
$\mathbf{2}^{2-}$	736 (67 700), 685(sh), 624(sh)
3	320 (12 800), 307(sh)
$\mathbf{3}^{\bullet-}$	692 (≈1900);[c] 355(sh); 319(≈5100)[c]
$[NPh_3]^{\bullet+\,b}$	650, 562; 358

[a] From spectroelectrochemistry in THF/0.1 M Bu_4NPF_6 at ambient temperature. [b] From irradiation in BuCl matrix.[9] [c] Approximate ϵ values (±10%) due to slow decomposition.

Chart 1

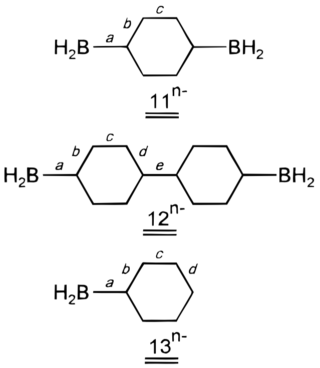

Table 3. Calculated[a] Bond Lengths *d* (Å) for Model Compounds **11**−**13**[b] and Their Anionic States

	d				
molecule	a	b	c	d	e
11	1.557	1.399	1.381		
$\mathbf{11}^{\bullet-}$	1.502	1.432	1.360		
$\mathbf{11}^{2-}$	1.459	1.475	1.342		
12	1.548	1.398	1.380	1.398	1.499
$\mathbf{12}^{\bullet-}$	1.504	1.421	1.362	1.430	1.433
$\mathbf{12}^{2-}$	1.467	1.453	1.344	1.471	1.370
13	1.549	1.400	1.383	1.387	
$\mathbf{13}^{\bullet-}$	1.534	1.425	1.377	1.394	
$\mathbf{13}^{2-}$	1.463	1.493	1.357	1.429	

[a] Optimized geometries using the 6-31G** basis, restricted HF method for open-shell systems. [b] For identification of bonds see Chart 1; $d_{BH} = 1.20 \pm 0.01$ Å.

reduction to the dianions, the similarly structured long-wavelength absorptions are shifted to higher energies—the typical behavior of conjugated redox systems.[1,2,11]

Calculations. *Ab initio* calculations with a 6-31G** basis were used for geometry optimization of the BH_2-substituted model redox systems $\mathbf{11}^{0/\bullet-/2-}$, $\mathbf{12}^{0/\bullet-/2-}$ and $\mathbf{13}^{0/\bullet-/2-}$ and for the fully substituted molecule $PhBMes_2$ (**3**). The calculated bond parameters (Chart 1) for the three redox systems are summarized in Table 3.

A comparison of the *ab initio* calculation results for **3** and **13** showed that the replacement of H by Mes does not affect the qualitative sequence of the relevant MOs. The only significant structural change involves the B−C(Ph) bond which increases to 1.593 Å for the bulkier molecule **3**. The calculated dihedral angle between Ph and Mes rings is 63.4°. The study of **3** and $\mathbf{3}^{2-}$ by the semiempirical AM1 method revealed a small decrease of the B−C(Mes) bonds (1.555 → 1.537 Å) but a large reduction of the B−C(Ph) bond length: 1.551 → 1.480 Å.

Whereas the LUMO energy of **13** is relatively high with 1.97 eV, the two diborane model species **11** (0.998 eV) and **12** (1.028 eV) do not differ much in that respect. The "redox orbital" which is occupied during stepwise reduction is of b_1 (**3**, **13**; C_{2v}) or b_{3u} symmetry (**11, 12**; D_{2h}). The contribution from the boron π centers to that MO amounts to 32.7 (**11**), 23.5 (**12**), and 35.2% (**13**). While the second unoccupied MOs (b_{2g}) of the diboranes **11** and **12** also have significant contribution from boron, the highest occupied molecular orbitals are π MOs of the aromatic rings.

Discussion

Experimental and Calculated Structures. The bond lengths and angles in **3** are very similar to those of other molecules with dimesitylboryl substituents.[6a−g,7h,11a] Despite the heavier substitution of benzene in structurally characterized 1,3,5-tris(dimesitylboryl)benzene (**10**),[6d] the tilting of the mesityl rings with respect to the phenyl plane is not very different here (71.9° in **3**; average of 70° in **10**[6d]). Assuming the usual $\cos^2$-dependence for the overlap between π orbitals, the interaction is clearly stronger in the boron−phenyl moiety ($\omega_1 = 21.5°$, $\cos^2 \omega_1 = 0.87$) than between the mesityl rings and π-accepting boron ($|\omega_2| = 60.6°$, $\cos^2 \omega_2 = 0.24$). As the crystallographically determined small structural changes between $BMes_3$ and $[BMes_3]^{\bullet-}$ have indicated,[6a] the conformation in such systems is largely determined by steric repulsion and the bond lengths are little affected due to π delocalization of the added electron.[5,6a]

In agreement with this notion, the *ab initio*-calculated Ph/Mes dihedral angle (63.4°) and the B−C(Ph) (1.593 Å) or B−C(Mes) distances (1.612 Å) are not very much different from the experimentally determined values (Figure 1). The different response of B−C(Ph) and B−C(Mes) bond lengths on reduction of **3** (AM1 calculations) confirm the primary localization of the added electrons in a π(phenyl)−p_z(B) based MO.

The calculations for the model redox systems $\mathbf{11}^{0/\bullet-/2-}$, $\mathbf{12}^{0/\bullet-/2-}$ and $\mathbf{13}^{0/\bullet-/2-}$ support the formulations in Scheme 2. For the diboranes there is a clear trend on successive one-electron reduction to quinonoid structures with localized single and double bonds, including the formation of borataalkene bonds with their typical[18] bond lengths of about 1.45 Å. Similarly alternant single/double bonds were observed in the structure of the dimesitylboryl-substituted 1,1′,4,4′-tetrahydrobipyridylidene (**7**);[12] a more balanced situation regarding bond lengths has been found in the all-carbon analogue **9** (Chichibabin's hydrocarbon).[13]

Spectroelectrochemistry. The near-UV absorption features between 300 and 350 nm of neutral complexes **1**−**3** can be assigned to HOMO−LUMO transitions between filled π molecular orbitals based on the aromatic rings and empty MOs with considerable boron participation.

The broad 692 nm absorption band following one-electron reduction of monoborane **3** compares well with the long-wavelength absorption at 650 nm for the related, i.e., isoelectronic, triphenylaminium radical cation.[9a] It is assigned to an electronic transition from the singly occupied molecular orbital (SOMO) b_1 to the next completely empty MO a_2, which has only a little contribution from boron. The HOMO−SOMO transition remains in the near-UV region.

The absorption spectrum of the *p*-phenylenediborane radical anion $\mathbf{1}^{\bullet-}$ (Figure 2) shows some resemblance to that reported for Wurster's Blue $\mathbf{4}^{\bullet+}$.[9b,10a] Intermolecular charge transfer transitions have frequently been discussed for Wurster's Blue

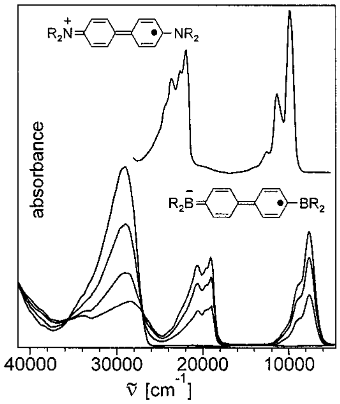

Figure 4. Absorption spectra of $\mathbf{5}^{\bullet+}$ (in BuCl matrix)[9c] and $\mathbf{2}^{\bullet-}$ (in THF/0.1 M Bu_4NPF_6). Note the wavenumber scale.

and related radical ions;[10] however, there can be no close intermolecular $\pi-\pi$ stacking in the borane species discussed here due to the steric bulk of the mesityl substituents. The long-wavelength band, accompanied by a shoulder, is attributed to an allowed SOMO−LUMO transition $b_{3u} \rightarrow b_{2g}$ (in spectroscopically effective D_{2h} symmetry of the chromophore), both of these π^* MOs being stabilized by the π-acceptor effect from two conjugated B centers in the *para* position. The remaining benzene π^* MO, a_u, remains unaffected (and hence unstabilized) due to the nodal plane in the 1,4-position.[19] The second intense band system of $\mathbf{1}^{\bullet-}$ at 424 nm is ascribed to a HOMO−SOMO transition $b_{1g} \rightarrow b_{3u}$.

The "mirror image" relation[5a] between amine and borane redox systems is most evident when comparing $\mathbf{2}^{\bullet-}$ with the tetramethylbenzidinium radical cation $\mathbf{5}^{\bullet+}$ (Figure 4).[9c,10b] There is a remarkable resemblance of band positions and band structures, extending even to small details of the well-visible vibrational structuring (Figure 4). Differences concern only the somewhat lower energy band positions and the additional occurrence of a (mesityl-based) absorption band at 346 nm for the borane system—both possibly substituent effects. The vibrational splitting with about 1200 cm^{-1} spacing is typical for polyaryl radical ions.[9−11] The assignment of the transitions is b_{3u}(SOMO) → b_{2g}(LUMO) for the 1305 nm band and b_{2g}(HOMO) → b_{3u}(SOMO) and b_{3u}(SOMO) → b_{1g}(SLUMO) for the band system around 500 nm.

Both the intensity and the long-wavelength position of the near-IR band of $\mathbf{2}^{\bullet-}$ are quite remarkable. The isoelectronic[4,12] radical cation $\mathbf{7}^{\bullet+}$ exhibits a similarly structured band[12a] albeit at a much shorter wavelength of 738 nm as compared to 1305 nm for $\mathbf{2}^{\bullet-}$.

The long-wavelength absorptions of the radical anions $\mathbf{1}^{\bullet-}$ and $\mathbf{2}^{\bullet-}$ may be alternatively described within the concept of metal-to-metal charge transfer in mixed-valent compounds.[20,21] The large contributions from the boron π centers to the redox orbitals as deduced from *ab initio* calculations (cf. above) and from previous EPR/ENDOR studies[5] allows us to regard these redox systems as π ligand-bridged diborane species. Assuming a B^{III}/B^{II} resonance structure (Scheme 3), the weaker coupling between the heteroelement centers across the larger biphenyl π system in $\mathbf{2}^{\bullet-}$ causes a long-wavelength shift for the transition between the symmetric (b_{3u}) and the antisymmetric (b_{2g}) combination[20c] of boron p_z orbitals. Since the intervening π systems act as π donors relative to the bridged heteroelement centers in $\mathbf{1}^{\bullet-}$ or $\mathbf{2}^{\bullet-}$, the situation does not resemble that of the Creutz−Taube ion[20c] but that of dianion-bridged dimetallic compounds with their typical extended π conjugation.[21] In contrast to such dimetalla π systems, the paramagnetic diborane intermediates provide p_π instead of d_π orbitals for conjugation.

In agreement with typical organic redox systems[11] and the polaron/bipolaron concept[17] the doubly reduced species $\mathbf{1}^{2-}$ and $\mathbf{2}^{2-}$ exhibit similarly structured, more intense, and hypsochromically shifted long-wavelength transitions $b_{3u} \rightarrow b_{2g}$ (HOMO−LUMO) in relation to the radical ion intermediates. Due to the complete filling of the b_{3u} "redox orbital" there are no more transitions possible to this MO. Nevertheless, the diborata-containing species $\mathbf{2}^{2-}$ exhibits again a significantly higher absorption wavelength (736 nm) than the related quinonoid molecules **7** (473 nm)[12a] or **9** (574 nm).[13]

Summarizing, we have demonstrated and supported with *ab initio* calculations that boron-based redox systems (Scheme 2) can be constructed as true "mirror images"[5a] of the widely used organonitrogen analogues (Scheme 1). The effective shielding required for the boron atoms may render these systems suitable for outer-sphere electron transfer applications at negative potentials (cf. eqs 1−3). In addition, the intense absorption features detected at very long wavelengths for the radical ion species could make these or similar systems interesting as near-IR dyes,[22] and the meta-substituted isomer of $\mathbf{1}^{2-}$ was recently characterized as a spin-unpaired triplet species with boron-centered spins.[23]

Acknowledgment. This work has been supported by grants from the Deutsche Forschungsgemeinschaft (DFG), Volkswagenstiftung, Fonds der Chemischen Industrie, and an Exchange Program between DFG and the Academy of Sciences of the Czech Republic.

Supporting Information Available: Tables of information on X-ray crystal data collection, anisotropic temperature factors, hydrogen atom coordinates, bond lengths and angles, and deviations from least-squares planes and figures of a stereoview and packing diagrams (9 pages). Ordering information is given on any current masthead.

IC951482W

---

(19) Heilbronner, E.; Bock, H. *The HMO Model and its Applications*: Verlag Chemie: Weinheim, Germany/Deerfield Beach, FL, 1976.

(20) (a) Blasse, G. *Struct. Bonding (Berlin)* **1991**, *76*, 153. (b) Prassides, K., Ed. *Mixed Valency Systems-Applications in Chemistry, Physics and Biology*; Kluwer: Dordrecht, The Netherlands, 1991. (c) Creutz, C.; Chou, M. H. *Inorg. Chem.* **1987**, *26*, 2995.

(21) (a) Kaim, W.; Kasack, V. *Inorg. Chem.* **1990**, *29*, 4696. (b) Kasack, V.; Kaim, W.; Binder, H.; Jordanov, J.; Roth, E. *Inorg. Chem.* **1985**, *34*, 1924.

(22) Fabian, J.; Zahradnik, R. *Angew. Chem.* **1989**, *101*, 693; *Angew. Chem., Int. Ed. Engl.* **1989**, *28*, 677.

(23) Rajca, A.; Rajca, S.; Desai, S. R. *J. Chem. Soc., Chem. Commun.* **1995**, 1957.